Introducing structural flexibility into porphyrin–DNA zipper arrays†

Ashley Brewer,[a] Guiliano Siligardi,[b,c] Cameron Neylon[d] and Eugen Stulz*[a]
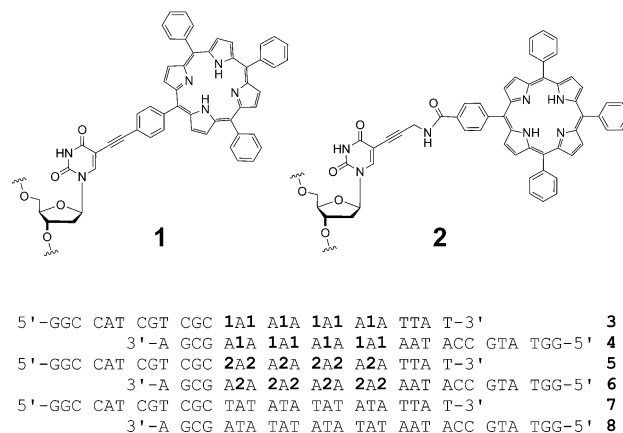
A more flexible nucleotide building block for the synthesis of new DNA based porphyrin–zipper arrays is described. Changing the rigid acetylene linker between the porphyrin substituent and the 2′-deoxyuridine to a more flexible propargyl amide containing linkage leads in part to an increased duplex stability. The CD spectra reveal different electronic interactions between the porphyrins depending on the type of linker used. Molecular modelling suggests large variation of the relative orientation of the porphyrins within the major groove of the DNA. The porphyrins can be metallated post-synthetically with different metals as shown with zinc, cobalt and copper. The spectroscopic features do not alter drastically upon metallation apart from the CD spectra, and the stability of the metal complex is highly dependent on the nature of the metal. As shown by CD spectroscopy, the zinc porphyrin is rapidly demetallated at high temperatures. Globular structure determination using SAXS indicates that a molecular assembly comprised of a two to four helical bundle dominates in solution at higher concentrations (≥50 µM) which is not observed by spectroscopy at lower concentrations (≤1 µM).

Introduction

The synthesis of electronically active organic molecules on the macromolecular scale[1] is of major interest due to their promising applications in light harvesting devices,[2] photovoltaics,[3] logic gates[4] and molecular wires.[5] The limiting factor in the development and refinement of these systems is often the speed of fabrication, since the introduction of a minor change to the final compound may dictate a completely different synthetic pathway. One solution to this is the development of modular building blocks, whereby the system as a whole can be tweaked and optimized through the relatively facile substitution of a different building block during the synthesis. Nature provides us with an abundant, easily modified[6,7] scaffold upon which to base our building blocks, namely DNA. A great deal of research has been conducted on modified DNA,[8–12] with many different electronically active molecules being covalently bound, for instance; pyrenes and perylenes,[13–16] and metallated bipyridines,[17,18] to name but a few. Many of these systems show efficient energy or electron transfer between donor and acceptor groups.[19–23] Our focus, however, is on the multiple attachments of porphyrins to the DNA scaffold. Porphyrins are an ideal choice for this purpose due to the facile tunability of their electronic properties through modification of the attached substituents or through metallation of the porphyrin macrocycle,[24] and they can easily be attached to a variety of scaffolds.[25–32] Other groups have used porphyrin–DNA constructs to create DNA bundles and tubes,[33,34] to form porphyrin dimers through hybridisation,[35] or as chiral markers for the analysis of DNA structure by CD spectroscopy.[36,37]

Previous research in our group has focused on tetraphenyl porphyrin (TPP, **1**)[38] or diphenyl porphyrin (DPP)[39] moieties connected *via* a rigid acetylene linker (Fig. 1).[40,41] Positioning all modifications on one strand leads to a destabilization of the duplex,[38,42] whereas when positioned on alternate strands (creating a zipper system) the modifications provide a significant degree of stabilization to the system,[11,43] similar to other reported zipper-DNA arrays.[44–46] Here we present a zipper–porphyrin system with a new linker to the nucleobase (**2**) which leads to a greater flexibility in the porphyrin arrangement, and explore different metallation states of the porphyrin arrays.


```
5'-GGC CAT CGT CGC 1A1 A1A 1A1 A1A TTA T-3'        3
       3'-A GCG A1A 1A1 A1A 1A1 AAT ACC GTA TGG-5'  4
5'-GGC CAT CGT CGC 2A2 A2A 2A2 A2A TTA T-3'        5
       3'-A GCG A2A 2A2 A2A 2A2 AAT ACC GTA TGG-5'  6
5'-GGC CAT CGT CGC TAT ATA TAT ATA TTA T-3'        7
       3'-A GCG ATA TAT ATA TAT AAT ACC GTA TGG-5'  8
```

Fig. 1 Acetylene (**1**) and amide (**2**) linked building blocks, and synthesized DNA strands.

Results and Discussion

Synthesis of the building blocks and porphyrin–DNA

The acetylene linked porphyrin building block **1** is readily obtained *via* Sonogashira coupling between the acetylene porphyrin and

[a] School of Chemistry, University of Southampton, Highfield, Southampton, UK, SO17 1BJ. E-mail: est@soton.ac.uk; Fax: +44-(0)23 80 59 68 05; Tel: +44-(0)23 80 59 93 69

[b] Diamond Light Source, Harwell Science and Innovation Campus, Didcot, Oxfordshire, UK, OX11 0DE

[c] School of Biological Sciences, University of Liverpool, Liverpool, UK, L69 3BX

[d] Science and Technology Facilities Council, Rutherford Appleton Laboratory, Harwell Science and Innovation Campus, Didcot, UK, OX11 0QX; Web: www.cameronneylon.net.

† Electronic supplementary information (ESI) available: Synthesis methods, molecular modelling, full spectroscopic analysis (UV-Vis, fluorescence and CD studies). See DOI: 10.1039/c0ob00535e

5-iodo-2′-deoxyuridine (5-I-dU).[38] To synthesize nucleotide **2**, first propargylamine is coupled to 5-I-dU to obtain the amine functionalised nucleoside (Scheme 1, Scheme S1, ESI†). It should be noted that protection of the propargylamine (*e.g.* with Fmoc) is not necessary. The coupling of the amino nucleoside with the corresponding monocarboxylic acid functionalised porphyrin proceeds smoothly using standard peptide coupling chemistry (EDC, HOBt, DMAP), and the amide linked porphyrin-dU is obtained in 80% yield. The free-base porphyrins were converted into the phosphoramidite nucleosides for automated DNA synthesis according to our protocols described earlier.[38,39] Fig. 1 lists the DNA strands that were synthesized in order to study the

influence of the new linker on structure and stability. The DNA single strands contain only one type of linker, *i.e.* an acetylene or an amide linker, but upon hybridization the different linkers can be mixed in the zipper arrays. Three porphyrin modified DNA duplexes were synthesised, where both strands contained either the acetylene linker (**3·4**) or the amide linker (**5·6**), and a hybrid system whereby one strand contained the acetylene linker while the other contained the amide linker (**3·6**). These systems have been designed to incorporate a 'sticky end' of eight bases at either end of the duplex for potential hybridization of other functional DNA strands.

Duplex stability of porphyrin–DNA

Two solvent systems (100% phosphate buffer and 9:1 phosphate buffer:DMF) were used for UV-Vis and fluorescence melting studies since discrete transitions for all systems in one solvent system were not observed; in some cases the melting transitions were much clearer when DMF was added to the system. The inclusion of 10% DMF in the buffer leads to a lowering of the duplexes' T_m (see **7·8**), ΔT_m values were calculated with respect to the unmodified duplex's (**7·8**) T_m in the appropriate solvent.

Unexpectedly a stabilising effect is observed in duplexes containing only one modified strand (**3·8**, **4·7**, **5·8** and **6·7**) and one natural complementary strand, which is observed in UV-melting and fluorescence-melting studies in both 100% buffered aqueous solvent and 9:1 buffer:DMF. The stabilization can be as large as +8.9 °C. The stabilizing effect of the porphyrins on these strands in aqueous buffer is 4.1 °C to 6.1 °C, while the same systems in 9:1 buffer:DMF show a stabilizing effect of 7.6 °C to 8.9 °C; the porphyrin modified DNA appears to be less sensitive to the destabilizing effect of DMF than natural DNA. Samples **5·8** and **6·7** also demonstrate that the difference in T_m between UV melting studies and fluorescence melting studies is 2–3 °C, with fluorescence melting studies giving the higher T_m value. The stabilizing effects observed here could indicate a favorable pre-organization of these strands towards the B-type duplex DNA. Porphyrins have been shown to be able to stabilize an induced helical structure in the single strands.[38] Interestingly this effect has a large positive effect on the duplex stability, presumably due to the attachment of the porphyrins onto alternating bases rather than in a continuous manner on each nucleotide as studied previously.[38]

The melting studies (Fig. 2 and Table 1) demonstrate a stabilising effect of +0.3 °C to +0.4 °C per porphyrin modification for duplexes containing two modified strands, presumably due to stacking interactions, which is in agreement with previous observations.[43] Overall, this leads to a stabilisation of around +4.5 °C in the porphyrin modified DNA duplexes compared to the natural DNA strand (**7·8**). The amide system (**5·6**) displays the largest ΔT_m, which may be caused by a stabilisation effect due to the introduction of flexibility within the system or due to the less sensitive nature of porphyrin DNA to DMF. However, a contribution of both factors is likely since the hybrid system (**3·6**) demonstrates a greater stabilising effect than the all acetylene system (**3·4**), due to the introduction of flexibility in some of the porphyrin modified nucleotides. In the UV-Vis spectra, porphyrin stacking interactions manifest themselves as a broadening of the porphyrin Soret band (B band) which, on heating above the duplex's T_m, narrows again; this is consistent with our previously
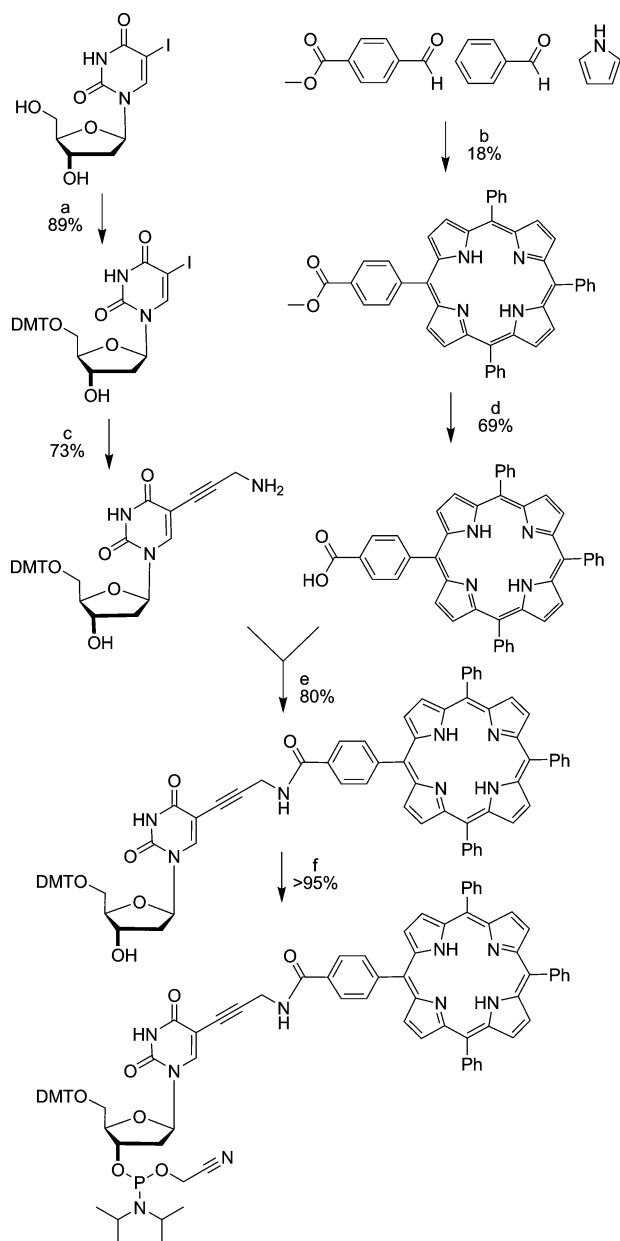

Scheme 1 Reagents and conditions: a) 4,4′-Dimethoxytrityl chloride, pyridine, CH₂CL₂; b) i) BF₃·Et₂O, CHCl₃, dark, ii) DDQ; c) propargylamine, Pd(PPh₃)₄, CuI, NEt₃, DMF; d) pyridine, KOH, H₂O, 40 °C; e) EDC, HOBt, DMAP, CH₂Cl₂, dark; f) (N(iPr)₂)P(Cl)OEtCN, DIPEA, CH₂Cl₂, dark.

Table 1 Melting temperatures of the porphyrin–DNA duplexes

	$T_m/°C^a$			
	Buffer	Buffer : DMF 9 : 1	$\Delta T_m/°C^d$	ΔT_m per porphyrin$/°C^d$
3·4	50.8^c	n.d.^{e}	3.6	0.3
5·6	n.d.^{e}	45.9^b	4.7	0.4
3·6	51.3^c	n.d.^{e}	4.1	0.3
7·8	47.2^b	41.2^b	—	—
3·8	53.3^c	n.d.^{e}	6.1	1.0
4·7	51.4^c	n.d.^{e}	4.1	0.7
5·8	51.8^c	46.2^b 48.8^c	4.6, 5.0, 7.6	0.8, 0.8, 1.3
6·7	52.1^c	47.3^b 50.1^c	4.9, 6.1, 8.9	0.8, 1.0, 1.5

^{a} buffer solution: 100 mM NaH_2PO_4/Na_2HPO_4, 100 mM NaCl, 1 mM Na_2-EDTA, pH 7.0, [DNA] = 1 μM; ^{b} UV melting; ^{c} fluorescence melting; ^{d} ΔT_m calculated with respect to the unmodified duplex (7·8); ^{e} no discrete transition detected.
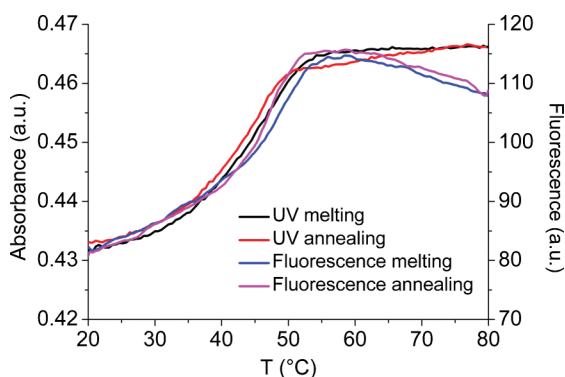
Fig. 2 UV and fluorescence melting curves of **5·8** as a representative example (9 : 1 buffer : DMF solution, conditions as in Table 1).

Fig. 3 a) CD spectra of the porphyrin regions of the duplexes **3·4**, **5·6** and **3·6**. b) CD spectra of the thermal demetallation of **3Zn** at 80 °C.

investigated porphyrin arrays. The different strands all exhibit identical spectroscopic behaviour, thus the linker does not have any influence on the electronic properties of the porphyrin. This also indicates that the porphyrin is electronically disconnected from the base stacking region of the DNA in all cases. Also, the 12-porphyrin systems do not show efficient energy transfer in steady-state fluorescence spectroscopy due to the unfavorable spectral overlap (*vide infra*); this is only observed in short porphyrin arrays.[43] Hysteresis of 3–5 °C between melting and annealing traces is observed in the UV and fluorescence thermal studies for all porphyrin modified duplexes, indicating differing kinetics of melting and annealing processes. A hysteresis of 1 °C or less is observed for the unmodified duplex (7·8), which would suggest that the melting and annealing transitions of porphyrin modified duplexes are different to the those undergone by 7·8.
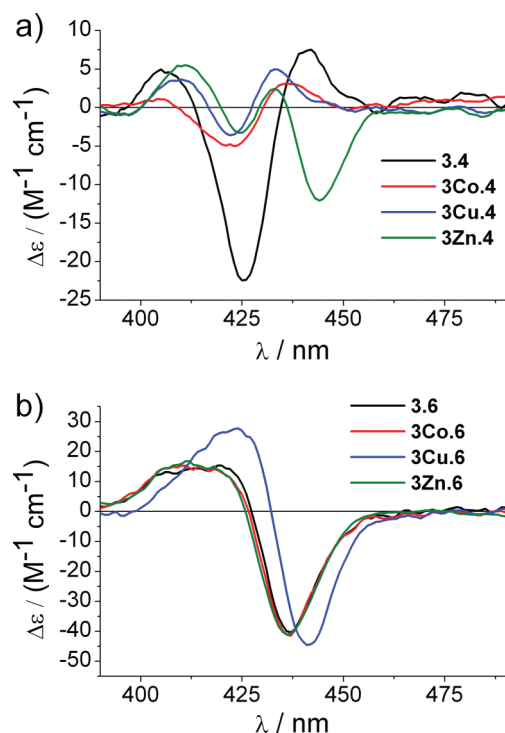
Circular dichroism spectroscopy of free base and metallated porphyrin–DNA

Circular dichroism (CD) spectroscopy showed the characteristic B-type DNA signatures for all duplexes, with a bisignate signal displaying maxima at λ = +276/−252 nm; little perturbation of these was observed for modified duplexes 3·4, 5·6 and 3·6, demonstrating that the conformation of the helix is not significantly altered even when modified with twelve porphyrins. Excitonic coupling of the porphyrin B band can be observed (Fig. 3a) in all samples. Duplexes containing the amide linked monomer (5·6 and 3·6) appear to act as linear oscillators, the B_x and B_y

transitions are not discrete and can be thought of as simple dipoles.[47] As such these give a simple −/+ bisignate spectrum (from longer wavelengths) with maxima at λ = −438/+419 nm and −436/+412 nm for 5·6 and 3·6 respectively. Duplex 3·4, containing only the shorter, more conformationally restricted acetylene linked monomer, gives a more complex +/−/+ trisignate signal at λ = +441/−425/+405 nm. The porphyrins in this system have to be considered as circular oscillators, that is, the perpendicular B_x and B_y transitions will both contribute significantly to the excitonic coupling. Multisignates of the Soret band have also been ascribed to π–π stacking between two close porphyrins when attached to a chiral scaffold with restricted conformational flexibility,[47] and this may also contribute to the CD band.

Facile metallation of strands 3 and 5 by zinc, cobalt and copper was achieved to give **xZn**, **xCo** and **xCu** (x = 3, 5), similar to previous work reported by Berova *et al.*[48] The strands were hybridized with 4 and 6 to form the alternating mixed metal-free base porphyrin arrays. Only small λ_{max} shifts of 2–7 nm were observed in the UV-Vis spectra upon metallation (Fig. S8, ESI†). The CD spectra of **5M^{2+}·6** were largely unaffected; however the systems **3M^{2+}·6** and **3M^{2+}·4** are more sensitive to metallation (Fig. 4), which could be due to a different porphyrin stacking along the DNA (*vide infra*). The duplex **3M^{2+}·4** seems particularly sensitive to metallation, and the CD bands show the most dramatic change compared to the corresponding free base porphyrin modified duplex. On metallation with cobalt or copper, the band remains as a +/−/+ trisignate with maxima at λ = +436/−423/+405 nm and +433/−422/+410 nm, respectively, but with a significant shift in peak maxima and intensities. In contrast, on metallation with

This journal is © The Royal Society of Chemistry 2011

*Org. Biomol. Chem.*, 2011, **9**, 777–782 | 779

a)

b)

Fig. 4 Comparison of the CD spectra of the metallated porphyrin–DNA strands **3·4** (a) and **3·6** (b).

zinc the trisignate becomes a $-/+/-/+$ tetrasignate signal ($\lambda = -444/+433/-425/+411$ nm). As has previously been mentioned, the CD bands of **3·4** are not a simple couplet and it is presumably these other interactions which cause the complexity of the CD band of **3Zn²⁺·4**. In these cases CD spectroscopy serves as a much better diagnostic tool to confirm metallation, as compared to UV-vis spectroscopy where only small differences were detected.

Here we also found that copper and cobalt metallated porphyrins are thermally stable up to 80 °C, but the zinc porphyrins are unstable at 80 °C, with a significant proportion reverting to the free base after 20 min (Fig. 3b). This effect is again much more pronounced in the CD spectra compared to the changes in absorbance. Zinc porphyrins have shown to be stable to demetallation up to 60 °C.

Molecular modelling

In order to detect differences in the relative orientation of the porphyrins as a function of the linker composition, molecular modelling was conducted on the duplexes **3·4**, **5·6** and **3·6** (Fig. 5). The energy minima were calculated from identical starting geometries (B-type DNA). The models predicted three very different structures with **3·4** and **5·6** both showing stacking of the porphyrins in a pairwise manner, with closest inter-porphyrin distances of 4.3 Å and 6.5 Å for **3·4**, and 4.4 Å and 7.9 Å for **5·6**. Pairwise stacking arises due to the modifications being bound to alternate strands with linkers of the same length, thus the porphyrins create two spirals in the major groove which are offset with respect to one another. This is not observed when all modifications are on the same strand.[38,39] The plane of the porphyrin rings in **3·4** are orientated at an angle of 71° with respect to the helical axis, while the plane of the porphyrin rings in **5·6** are
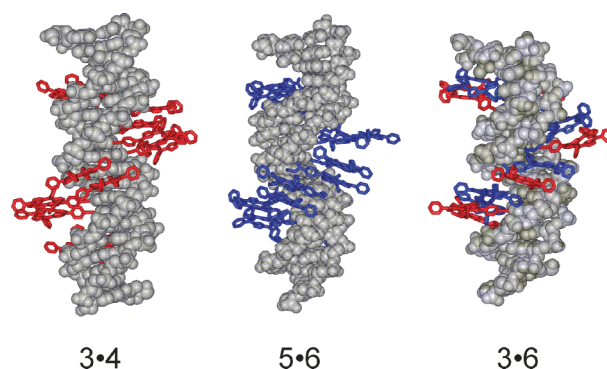

Fig. 5 Molecular modelling of porphyrin–DNA zipper systems (Macro-Model, AMBER*).[49]

oriented at an angle of 110° to the helical axis. Interestingly, when the two different linkers are combined in the duplex **3·6**, pairwise stacking is no longer pronounced, with closest inter-porphyrin distances of 4.5 Å and 5.5 Å. Also the plane of the porphyrin rings is nearly perpendicular to the helical axis, at an angle of 94°, giving the appearance of a slipped stack and predicting a much better fit in the duplex. In contrast to what might be predicted from the models, the more even distribution of the porphyrins in **3·6**, which would provide more even interstrand interactions across the length of the modified section of the duplex, does not lead to a significantly enhanced stabilisation of the duplex.

Solution phase association

The overall structure of the DNA construct in solution was examined for **3·4** using laboratory small angle X-ray scattering (SAXS). The data were consistent with an elongated monodisperse aggregate. The simplest model to provide an adequate fit is a cylinder with a length of 13 nm and a radius of 3.9 nm (Fig. 6a). While the length is consistent with that predicted from the modelling of the DNA, the radius suggests an association complex of two to four double helices forming in solution. We propose a model for the formation of a two to four helical bundle as shown in Fig. 6a, which seems to dominate at higher concentrations and is most likely induced by weak hydrophobic intermolecular interactions between the porphyrins. Similar formation of higher order assemblies induced by porphyrin–porphyrin interactions in DNA have recently been reported to occur at high ionic strength.[37] According to the SAXS data, these helical bundles are discrete entities, and solubility is not affected by this molecular association; no precipitation or light scattering was observed. It should be noted that the SAXS experiments were performed at a rather high concentration of 50 µM. The spectroscopic data (absorbance, CD) are distinctly different at high concentration (Fig. 6b) compared to low concentration. At 56 µM, the absorbance shows a clear maximum at $\lambda = 419$ nm and a shoulder at $\lambda \sim 409$ nm, whereas at 1 µM the absorbance is very broad ($\lambda_{max} = 410$ nm). The CD spectrum appears sharper and more intense in the normalised spectrum, but most notably the bisignate spectrum changes to a trisignate spectrum. These differences suggest that the intermolecular interactions occur only at higher concentrations, and that the spectroscopic data (absorbance, CD) discussed above reflect the single porphyrin–DNA behaviour rather than that of the aggregates.
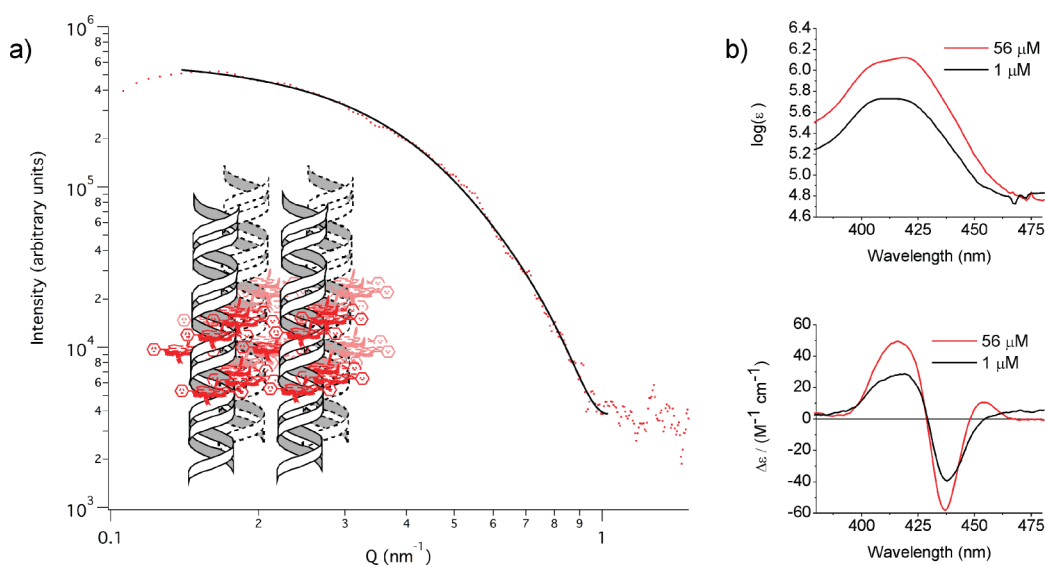
Fig. 6 a) SAXS data recorded on a solution of porphyrin modified DNA (**3·4**) at 50 µM. The fit is to a simple rigid cylinder with a radius of 3.9 nm and a length of 13 nm, which is consistent with a two to four helical bundle; b) Absorbance (top) and CD (bottom) spectra of **3·4** at both 56 µM and 1 µM concentration.

Conclusions

To summarize, we have demonstrated the synthesis of zipper-like porphyrin modified DNA containing two different linkers. The arrays contain 12 porphyrins and span a full helical turn, where the inter-porphyrin distance and torsion angles with respect to the helical axis are dependant on the linker incorporated. The porphyrins are easily metallated post-synthetically with various 3d transition metals. The complexes' thermal stability varies between metals with Co(II) and Cu(II) being stable but Zn(II) being unstable and reverting back to the free base within minutes at 80 °C. The duplexes studied seem to adopt markedly different conformations of the porphyrins within the major groove of the DNA, shown by CD and molecular modelling. Using the same linker in both strands results in a pairwise stacking of the porphyrins, whereas the hybrid systems give a more even distribution of the porphyrins. However, this does not affect the spectroscopic properties, and the differences are probably too subtle to be detected. The thermal stability of the duplexes, on the other hand, are dependent on the structure of the linker and the nature of the solvent. The precise arrangement of large hydrophobic substituents within the major groove of the DNA is therefore a very important factor in determining the stability of modified DNA. It should also be noted that the porphyrin–DNA systems tend to associate to higher ordered arrays at higher concentrations, which might also be the case for other synthetic DNA systems which bear hydrophobic groups. The systems are now under investigation for their photoinduced electron transfer efficiency and ability to perform as electronic wires.

Acknowledgements

Notes and references

1 E. Schwartz, S. Le Gac, J. Cornelissen, R. J. M. Nolte and A. E. Rowan, *Chem. Soc. Rev.*, 2010, **39**, 1576–1599.
2 D. Furutsu, A. Satake and Y. Kobuke, *Inorg. Chem.*, 2005, **44**, 4460–4462.
3 H. Imahori, *J. Mater. Chem.*, 2007, **17**, 31–41.
4 S. D. Straight, J. Andreasson, G. Kodis, S. Bandyopadhyay, R. H. Mitchell, T. A. Moore, A. L. Moore and D. Gust, *J. Am. Chem. Soc.*, 2005, **127**, 9403–9409.
5 Y. H. Kim, D. H. Jeong, D. Kim, S. C. Jeoung, H. S. Cho, S. K. Kim, N. Aratani and A. Osuka, *J. Am. Chem. Soc.*, 2001, **123**, 76–86.
6 F. W. Hobbs, *J. Org. Chem.*, 1989, **54**, 3420–3422.
7 V. Borsenberger, M. Kukwikila and S. Howorka, *Org. Biomol. Chem.*, 2009, **7**, 3826–3835.
8 V. L. Malinovskii, D. Wenger and R. Häner, *Chem. Soc. Rev.*, 2010, **39**, 410–422.
9 M. Endo and H. Sugiyama, *ChemBioChem*, 2009, **10**, 2420–2443.
10 R. Varghese and H. A. Wagenknecht, *Chem. Commun.*, 2009, 2615–2624.
11 H. A. Wagenknecht, *Angew. Chem., Int. Ed.*, 2009, **48**, 2838–2841.
12 T. J. Bandy, A. Brewer, J. R. Burns, G. Marth, T. Nguyen and E. Stulz, *Chem. Soc. Rev.*, 2010, DOI: 10.1039/B820255A.
13 J. Barbaric and H. –A. Wagenknecht, *Org. Biomol. Chem.*, 2006, **4**, 2088–2090.
14 E. Mayer-Enthart and H.-A. Wagenknecht, *Angew. Chem., Int. Ed.*, 2006, **45**, 3372–3375.
15 D. Lindegaard, A. S. Madsen, I. V. Astakhova, A. D. Malakhov, B. R. Babu, V. A. Korshun and J. Wengel, *Bioorg. Med. Chem.*, 2008, **16**, 94–99.
16 M. V. Skorobogatyi, A. D. Malakhov, A. A. Pchelintseva, A. A. Turban, S. L. Bondarev and V. A. Korshun, *ChemBioChem*, 2006, **7**, 810–816.
17 M. Vrabel, P. Horakova, H. Pivonkova, L. Kalachova, H. Cernocka, H. Cahova, R. Pohl, P. Sebest, L. Havran, M. Hocek and M. Fojta, *Chem.-Eur. J.*, 2009, **15**, 1144–1154.
18 M. Kalek, A. S. Madsen and J. Wengel, *J. Am. Chem. Soc.*, 2007, **129**, 9392–9400.
19 M. Fukuda, M. Nakamura, T. Takada and K. Yamana, *Tetrahedron Lett.*, 2010, **51**, 1732–1735.

20 N. A. Grigorenko and C. J. Leumann, *Chem. Commun.*, 2008, 5417–5419.

21 R. Varghese and H. A. Wagenknecht, *Chem.–Eur. J.*, 2009, **15**, 9307–9310.

22 H. Kashida, T. Takatsu, K. Sekiguchi and H. Asanuma, *Chem.–Eur. J.*, 2010, **16**, 2479–2486.

23 H. Kashida, K. Sekiguchi, X. Liang and H. Asanuma, *J. Am. Chem. Soc.*, 2010, **132**, 6223–6230.

24 K. Kalyanasundaram, *Photochemistry of Polypyridine and Porphyrin Complexes*, Academic Press, London, 1992.

25 Y. S. Nam, T. Shin, H. Park, A. P. Magyar, K. Choi, G. Fantner, K. A. Nelson and A. M. Belcher, *J. Am. Chem. Soc.*, 2010, **132**, 1462–1463.

26 I. Beletskaya, V. S. Tyurin, A. Y. Tsivadze, R. Guilard and C. Stern, *Chem. Rev.*, 2009, **109**, 1659–1713.

27 G. J. E. Davidson, L. A. Lane, P. R. Raithby, J. E. Warren, C. V. Robinson and J. K. M. Sanders, *Inorg. Chem.*, 2008, **47**, 8721–8726.

28 K. M. Mullen and M. J. Gunter, *J. Org. Chem.*, 2008, **73**, 3336–3350.

29 F. D'Souza and O. Ito, *Chem. Commun.*, 2009, 4913–4928.

30 S. Fukuzumi, T. Honda, K. Ohkubo and T. Kojima, *Dalton Trans.*, 2009, 3880–3889.

31 G. A. Metselaar, P. Ballester and J. de Mendoza, *New J. Chem.*, 2009, **33**, 777–783.

32 R. W. Seidel and I. M. Oppel, *Z. Anorg. Allg. Chem.*, 2010, **636**, 446–448.

33 M. Endo, N. C. Seeman and T. Majima, *Angew. Chem., Int. Ed.*, 2005, **44**, 6074–6077.

34 M. Endo, T. Shiroyama, M. Fujitsuka and T. Majima, *J. Org. Chem.*, 2005, **70**, 7468–7472.

35 M. Endo, M. Fujitsuka and T. Majima, *J. Org. Chem.*, 2008, **73**, 1106–1112.

36 A. D'Urso, A. Mammana, M. Balaz, A. E. Holmes, N. Berova, R. Lauceri and R. Purrello, *J. Am. Chem. Soc.*, 2009, **131**, 2046–2047.

37 A. Mammmana, G. Pescitelli, T. Asakawa, S. Jockusch, A. G. Petrovic, R. R. Monaco, R. Purrello, N. J. Turro, K. Nakanishi, G. A. Ellestad, M. Balaz and N. Berova, *Chem.–Eur. J.*, 2009, **15**, 11853–11866.

38 L. A. Fendt, I. Bouamaied, S. Thöni, N. Amiot and E. Stulz, *J. Am. Chem. Soc.*, 2007, **129**, 15319–15329.

39 I. Bouamaied, T. Nguyen, T. Rühl and E. Stulz, *Org. Biomol. Chem.*, 2008, **6**, 3888–3891.

40 I. Bouamaied and E. Stulz, *SYNLETT*, 2004, 1579–1583.

41 I. Bouamaied and E. Stulz, *Chimia*, 2005, **59**, 101–104.

42 I. Bouamaied, L. A. Fendt, M. Wiesner, D. Häussinger, S. Thöni, N. Amiot and E. Stulz, *Nucleosides, Nucleotides Nucleic Acids*, 2007, **26**, 1533–1538.

43 T. Nguyen, A. Brewer and E. Stulz, *Angew. Chem., Int. Ed.*, 2009, **48**, 1974–1977.

44 D. Baumstark and H. A. Wagenknecht, *Chem.–Eur. J.*, 2008, **14**, 6640–6645.

45 M. D. Sorensen, M. Petersen and J. Wengel, *Chem. Commun.*, 2003, 2130–2131.

46 C. Brotschi and C. J. Leumann, *Angew. Chem., Int. Ed.*, 2003, **42**, 1655–1658.

47 G. Pescitelli, S. Gabriel, Y. K. Wang, J. Fleischhauer, R. W. Woody and N. Berova, *J. Am. Chem. Soc.*, 2003, **125**, 7613–7628.

48 A. Mammana, T. Asakawa, K. Bitsch-Jensen, A. Wolfe, S. Chaturantabut, Y. Otani, X. X. Li, Z. M. Li, K. Nakanishi, M. Balaz, G. A. Ellestad and N. Berova, *Bioorg. Med. Chem.*, 2008, **16**, 6544–6551.

49 F. Mohamadi, N. G. J. Richards, W. C. Guida, R. Liskamp, M. Lipton, C. Caufield, G. Chang, T. Hendrickson and W. C. Still, *J. Comput. Chem.*, 1990, **11**, 440–467.